NOMA VLC Systems and Neural Network Approach for Imperfect SIC

Mahesh Kumar Jha[1,2], Navin Kumar[3], Rubini P.[4], and Y. V. S. Lakshmi[5]
[1] Research Scholar, CMR University, Bengaluru, Karnataka, India
[2] Dept. of ECE, CMR Institute of Technology, Bengaluru, Karnataka, India
[3] Dept. of ECE, Amrita School of Engineering, Bengaluru India
[4] Dept. of CSE, School of Engineering and Technology, CMR University, Bengaluru, Karnataka, India
[5] Centre for Development of Telematics, Bengaluru, India
Email: mahesh.kumarjha.in@ieee.org; navin_kum3@yahoo.com; rubini.p@cmr.edu.in; lakshmi@cdot.in

Abstract—Non Orthogonal Multiple Access (NOMA) technique in Visible Light Communications (VLC) enhances the performances like spectral efficiency, achievable data rate, fairness, outage probability, etc. NOMA uses superposition in power domain at the transmitter and Successive Interference Cancellation (SIC) at the receiver. SIC operation is expected to perform perfect cancellation to avoid errors in the received signal. In this paper, Neural Network (NN) methods are used to overcome imperfect SIC in a NOMA VLC system. The Signal to Noise Ratio (SNR), Bit Error Rate (BER), and bitrate performance of the NOMA VLC systems are analyzed using Convolution Neural Network (CNN), long short term memory (LSTM), and Deep Neural Network (DNN) algorithms. Simulation results shows that the NN methods outperforms the conventional NOMA VLC system to a perfect SIC. Considering SNR for the BER 10^{-4}, CNN outperforms SIC by 5 dB, DNN by 2 dB and LSTM by 1.5 dB. Further, CNN also outperforms SIC, DNN, and LSTM based NOMA VLC systems for BER performance as a function of bitrate. Thus, NN-based receiver will be a better alternative for imperfect SIC.

Index Terms—NOMA, Convolution Neural Network (CNN), Long Short Term Memory (LSTM), and Deep Neural Network (DNN), Successive Interference Cancellation (SIC)

I. INTRODUCTION

Recently, visible light communication (VLC) has shown high potential and received high attention from research community for short communication in 5G and beyond [1]. Many techniques that are used widely in radio frequency (RF) systems are being implemented/tested in VLC but still VLC faces challenges while dealing with multiple access (MA).

Multiple access technique is must to support multi user in VLC. The orthogonality property of MA including code division multiple access (CDMA), time division multiple access (TDMA), and orthogonal frequency division multiple access (OFDMA) was implemented in VLC to overcome users interference [2], [3]. As a result, lower interference is achieved at the cost of achievable data rate with spectral efficiency and fairness. Non-orthogonal Multiple Access (NOMA) is proposed in VLC to synchronize fairness, spectral efficiency, and throughput [4], [5].

In NOMA, user has orthogonal access either in time, frequency, code or space and same band is used by each user to operate at the same time in power domain [6]. NOMA applies superposition coding at the transmitter to transmit the signal and Successive Interference Cancellation (SIC) at the receiver to decode the signal. Unlike RF, in VLC superposition coding uses channel knowledge for each user to split the power between them. Different Power Allocation (PA) techniques have been proposed for NOMA-VLC [7]-[10]. The gain ratio power technique is proposed in [7] where users channel conditions ensure fair PA. In [8], PA is based on user grouping technique. In [9], PA is proposed to optimize sum rate and fairness while PA for mobile users are considered in [10].

In NOMA based VLC systems, SIC receiver performance depends on perfect cancellation for decoding the users signal but achieving a perfect cancellation is very challenging because any mismatch will lead to error in decoding [11]. In addition, VLC also suffers nonlinear distortion at the transmitter, channel, and photo diodes at the receiver, due to the nonlinearity characteristics of LEDs [12]. The nonlinearity affects the system performance especially Bit Error Rate (BER). The nonlinearity mitigation techniques have been investigated to overcome few simple effects but complexity at the hardware was not addressed.

Recently, Neural Network (NN) has been identified as an efficient tool for end to end communication [13] especially when input output relationship of a system is nonlinear. In [14], NN is used to train and predict the nonlinearity of VLC. The channel estimation is also monitored using NN algorithms [15], [16].

This paper presents a NOMA VLC system which has been analyzed using conventional method and NN based algorithms. The proposed contributions are as follows:

- NOMA based VLC system is analyzed to evaluate performance parameters such as achievable data

Manuscript received April 1, 2021; revised August 17, 2022.
doi:10.12720/jcm.17.9.723-733

rate, outage probability, signal to noise ratio (SNR), BER, and fairness.

- Additionally, fair PA (FPA) and modified fair PA (MFPA) techniques for dynamic power allocation (DPA) are proposed based on required sum rate. The performance is compared with static PA (SPA) technique.
- Further, the NOMA VLC system is analyzed using NN algorithms, Convolution Neural Network (CNN), Long Short Term Memory (LSTM), and Deep Neural Network (DNN) are considered to analyze the SNR, BER, and bitrate performance of the NOMA VLC system. Simulation results shows that the implementation of NN methods outperform the conventional SIC based NOMA VLC system. SIC operations should perform perfect cancellation to avoid errors in received signal to resolve the issue of imperfect SIC, NN-based receiver can be used.

The rest of the paper is organized as follows. Section II discusses a NOMA VLC system model. The proposed scenario for this work is described in Section III. Section IV explains and analyzes NN algorithm. The results are discussed in Section V and finally, conclusion is made in Section VI.

II. A NOMA VLC SYSTEM MODEL

The conventional NOMA VLC system is shown in Fig. 1(a)-(c). Consider multi user VLC system in an indoor room with total number of users U. The user's serial bit stream is converted into parallel. The 4-quadrature amplitude modulation (QAM) mapping is performed on these parallel data and symbols are mapped to N subcarriers. Then, real time domain signals are obtained by applying $N/2$ subcarriers and inverse fast Fourier transform (IFFT). The $(N/2-1)$ subcarriers are used to communicate unique information and the subcarriers $S(0)$ and $S(N/2)$ are set to zero which does not carry any information. The N-IFFT frame structure S is represented as:

$$S = \{0, S(1), S(2), .., S\left(\frac{N}{2}-1\right), 0, S^*\left(\frac{N}{2}-1\right), .., S^*(2), S^*(1)\}^T \quad (1)$$

The output of N-IFFT and power allocation in time domain is represented by s_i and p_i respectively for user i ($i = 1, 2, .., U$). According to the NOMA principle, power p_i is allocated to messages s_i corresponding to all users and superposition is performed in the power domain. The superposed signal is DC biased to obtain non-negative before transmitting through the LEDs.

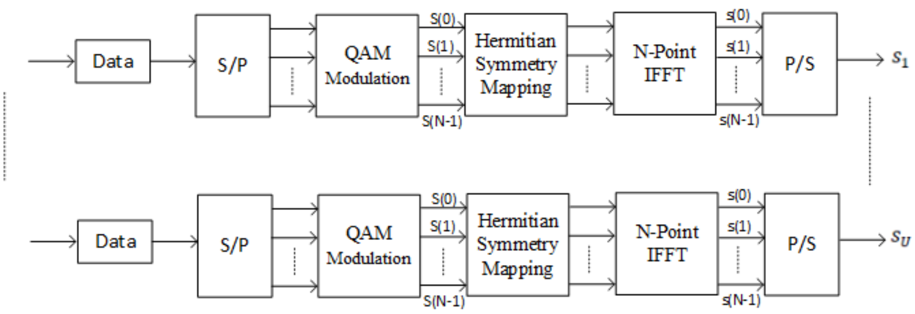

Fig. 1(a). NOMA VLC transmitter

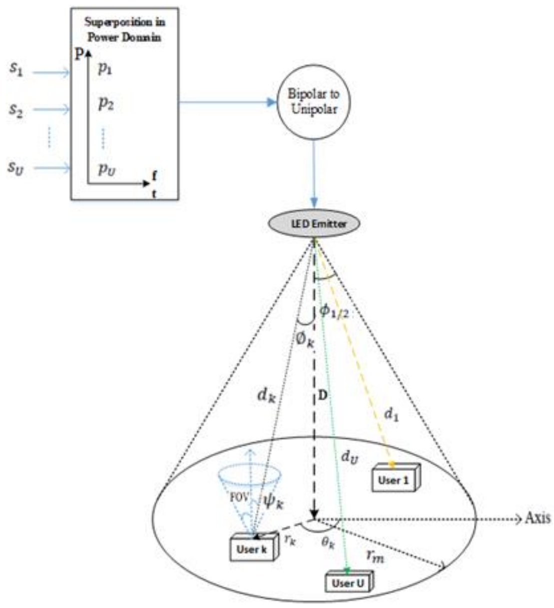

Fig. 1(b). Optoelectronic scenario

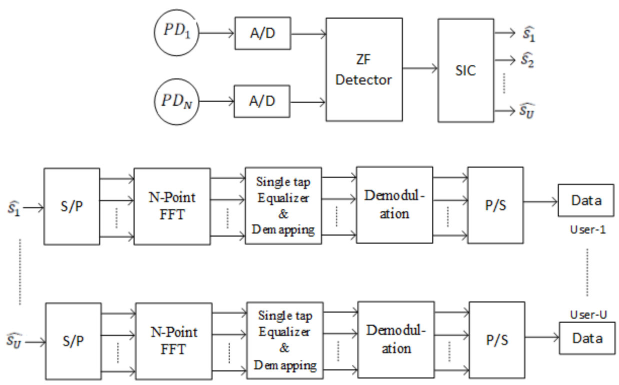

Fig. 1(c). NOMA-VLC receiver

The signal transmitted through LEDs is given as:

$$x = \sum_{i=1}^{U} C_i \sqrt{P_{TE}} S_i + I_{DC} \quad (2)$$

P_{TE}: Total electrical power,
C_i : PA coefficient for i^{th} user,
S_i : Modulated message signal intended for the i^{th} user;

I_{DC}: DC bias added to ensure the positive instantaneous intensity

C_i is greater for the user having poor channel gain or located far from the emitters. Consider user U is farthest and user 1 is nearest.

$$C_1 \leq C_2 \leq C_3 \dots \dots C_k \dots \leq C_U \tag{3}$$

Also, $$\sum_{i=1}^{U} C_i^2 = 1 \tag{4}$$

The PA factor (λ) is given as:

$$\lambda = \frac{C_i^2}{C_{i-1}^2},\ i = 2, \dots\dots, k, \dots., U \tag{5}$$

The signal x is transmitted through LED emitters and received by the user's device equipped with photodiodes (PDs). The reflections from ceiling, floor, and walls are not quantitatively strong, hence only line of sight (LoS) path is considered. The DC channel gain [17] using LoS for k^{th} user is given as:

$$h_k = \begin{cases} \frac{(m+1)rA}{2\pi d_k^2} cos^m(\emptyset_k) cos(\psi_k)\alpha\beta,\ 0 \leq \psi_k \leq \text{FOV} \end{cases} \tag{6}$$

The parameters detail as given below:

$m = -\ln(2)/\ln(\cos(\Phi_{1/2})$: Order of Lambertian radiation pattern of LED.

$\Phi_{1/2}$: Semi angle of LED at half power.

A and r: PD's active area and responsivity.

ψ_K: Angle of incidence for k^{th} user.

$\emptyset_K$: Angle of irradiance for k^{th} user.

d_K: Distance between LED emitter and k^{th} user.

α & β: gain of optical filter and concentrator at the receiver respectively.

FOV: field of view (FOV) of PD.

From (3) and without loss of generality, channel gains are arranged for the users as:

$$h_1 \geq h_2 \geq h_3 \dots \dots \geq h_k \dots \geq h_U \tag{7}$$

The channel gain is zero if incident light is out of FOV range.

The unipolar signal is transmitted by LEDs and received by PDs of the user device at the receiver. The received signal at k^{th} user after DC removal is given by:

$$y_k = \sqrt{P_{TE}} h_k \left(\underbrace{\sum_{j=1}^{k-1} C_j S_j}_{\text{SIC}} + \underbrace{C_k S_k}_{\text{Signal}} + \underbrace{\sum_{j=k+1}^{U} C_j S_j}_{\text{Interference}} \right) + W_k \tag{8}$$

W_k: Additive white Gaussian noise (AWGN)

The received signal is converted into digital before passing through zero forcing (ZF) detector. ZF is used with channel inversion because of low complexity. By using this, k^{th} user estimated signal is given as:

$$\widehat{x_k} = x + \frac{1}{rP_o} {h_K}^{-1} W_K \tag{9}$$

where, P_o is the optical power of LED.

Next, SIC is performed as per NOMA principle to decode s_K. $\widehat{s_k}$ is the estimated value of s_K as indicated in Fig. 1(c). SIC is an iterative process to decode the data in the decreasing order of power levels. The data of user who has assigned highest power or farthest from emitter is decoded first. Then, the data of the user who has given the next highest power is decoded. According to (3) & (7), first s_U is decoded. While decoding the data of one user, the other signals will be recognized as a noise. To decode the next user's data, s_U is subtracted from the received signal considering, signals with higher channel gains as a noise and this process repeats till decoding is done for all user's data. Equation (8) shows the required signal for k^{th}user with interference and SIC.

The achievable data rate for k^{th} user as per Shannon's theorem is given as:

$$R_k = \begin{cases} \frac{B}{2} log_2\left(1 + \frac{(h_k C_k)^2}{\sum_{i=1}^{k-1}(h_k C_i)^2 + \sum_{j=k+1}^{U}\left(h_k C_j\right)^2 + \frac{1}{\rho}}\right) \\ \qquad for\ k = 1,2, \dots U-1 \\ \frac{B}{2} log_2\left(1 + \frac{(h_k C_k)^2}{\sum_{i=1}^{k-1}(h_k C_i)^2 + \frac{1}{\rho}}\right) \quad for\ k = U \end{cases} \tag{10}$$

where, $\rho = P_{TE}/N_o B$, N_o is noise spectral density, B is Bandwidth, and 1/2 is constraint of Hermitian symmetry. The sum capacity (R_T) and fairness index (F) is given as:

$$R_T = \sum_{k=1}^{U} R_k \tag{11}$$

$$F = \frac{(\sum R_k)^2}{U \sum R_k^2} \tag{12}$$

here F represent the fairness of the system capacity among the users.

The PA is one of the key features in NOMA. The objective of the PA is to maximize the R_T under a constraint of F for NOMA systems. The optimization problem is then formulated as:

Maximize R_k and λ

Subject to:

$$\sum_{k=1}^{U} P_k \leq P_{TE}, \quad P_k \geq 0, \forall k, \quad F = F' \tag{13}$$

F': The target fairness index.

III. Proposed Scenario

Consider a room $6m \times 6m \times 3m$ as shown in Fig. 2 in which one LED emitter is placed on the ceiling to provide the service for two users. It is further assumed that user 2 is far and user 1 is near.

Signals transmitted through LED using NOMA is given as:

$$x = \sqrt{P_{TE}}(C_{1n}S_1 + C_{2f}S_2) + I_{DC} \tag{14}$$

C_{2f} = PA coefficient for far user

C_{1n} = PA coefficient for near user

At the receiver, y_1 and y_2 is received signal at user-1 and user-2 respectively represented as:

$$y_1 = h_{1n}x + W_1 \tag{15}$$

$$y_2 = h_{2f}x + W_2 \tag{16}$$

h_{2f} = channel coefficient for far user

h_{1n} = channel coefficient for near user

After DC removal, y_1 and y_2 can be expressed as:

$$y_1 = \underbrace{h_{1n}\sqrt{P_{TE}}C_{1n}S_1}_{\text{desired signal}} + \underbrace{h_{1n}\sqrt{P_{TE}}C_{2f}S_2}_{\text{interference}} + \underbrace{W_1}_{\text{noise}} \tag{17}$$

$$y_2 = \underbrace{h_{2f}\sqrt{P_{TE}}C_{1n}S_1}_{\text{interference}} + \underbrace{h_{2f}\sqrt{P_{TE}}C_{2f}S_2}_{\text{desired signal}} + \underbrace{W_2}_{\text{noise}} \tag{18}$$

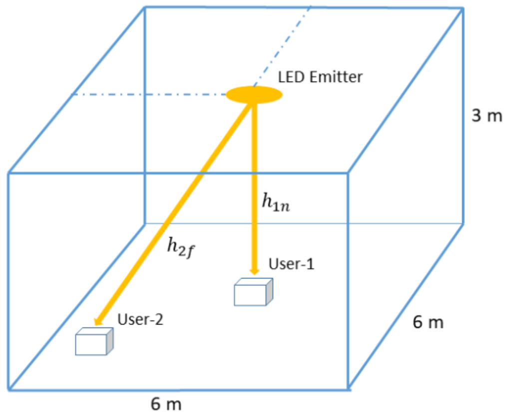

Fig. 2. Room layout

Considering perfect and imperfect cancellation under SIC, User-2 (far user) data is decoded first and user-1 (near user) performs SIC before decoding his own signal. By assuming perfect cancellation with user-1 data, the y_1 after SIC will be represented as:

$$y_1 = h_{1n}\sqrt{P_{TE}}C_{1n}S_1 + h_{1n}\sqrt{P_{TE}}C_{2f}S_2 + W_1 - h_{1n}\sqrt{P_{TE}}C_{2f}S_2$$

$$y_1 = h_{1n}\sqrt{P_{TE}}C_{1n}S_1 + W_1 \tag{19}$$

Considering imperfect cancellation which means that some fraction of S_2 is present in $y_1$after SIC in the user-1 data then, y_1 after SIC will be represented as:

$$y_1 = h_{1n}\sqrt{P_{TE}}C_{1n}S_1 + \sqrt{\epsilon}\, h_{1n}\sqrt{P_{TE}}C_{2f}S_2 + W_1 \tag{20}$$

where ϵ is the fraction of S_2.

The achievable data rate for perfect SIC is calculated as:

$$R_{2f} = \frac{B}{2}log_2\left(1 + \frac{(h_{2f}C_{2f})^2 P_{TE}}{(h_{2f}C_{1n})^2 P_{TE} + \sigma^2}\right) \tag{21}$$

$$R_{1n} = \frac{B}{2}log_2\left(1 + \frac{(h_{1n}C_{1n})^2 P_{TE}}{\sigma^2}\right) \tag{22}$$

For imperfect SIC,

$$R_{1n} = \frac{B}{2}log_2\left(1 + \frac{(h_{1n}C_{1n})^2 P_{TE}}{\epsilon(h_{1n}C_{2f})^2 P_{TE} + \sigma^2}\right) \tag{23}$$

R_{1n} is obtained after removing the interference from far user transmission by SIC. Noise power is given as $\sigma^2 = N_o B$.

$$(C_{2f})^2 + (C_{1n})^2 = 1,\ \ C_{2f} > C_{1n} \tag{24}$$

Outage probability:

The signal to interference noise ratio (SINR) for the far user is:

$$\gamma_{2f} = \frac{(h_{2f}C_{2f})^2 P_{TE}}{(h_{2f}C_{1n})^2 P_{TE} + \sigma^2} \tag{25}$$

The SINR at the user 1 for decoding the user 2 signal (before SIC) is

$$\gamma_{2f\to 1n} = \frac{(h_{1n}C_{2f})^2 P_{TE}}{(h_{1n}C_{1n})^2 P_{TE} + \sigma^2} \tag{26}$$

The SINR for the near user is:

$$\gamma_{1n} = \frac{(h_{1n}C_{1n})^2 P_{TE}}{\sigma^2} \tag{27}$$

User-1 is not in outage, if it decodes both signals S_1 and S_2 received from x. The outage probability at user-1 is given as:

$$Outage\ probability_{1n} = 1 - Prob(\gamma_{2f\to 1n} > \gamma_2, \gamma_{1n} > \gamma_1) \tag{28}$$

where $\gamma_2 = 2^{2R_2/B} - 1$ and $\gamma_1 = 2^{2R_1/B} - 1$; R_1 and R_2 are the desired data rate for user-1 and user-2 respectively.

User-2 is in outage, if SIC cannot decode the S_2 received from x or user-2 cannot decode S_2 forwarded by SIC.

The outage probability at user-2 is given as:

$$Outage\ probability_{2f} = 1 - Prob(\gamma_{S_2} > \gamma_2, \gamma_{2f} > \gamma_2) \tag{29}$$

where, γ_{S_2} is the SINR to decode S_2.

IV. Dynamic Power Allocation (DPA)

DPA can be achieved by maximizing the sum rate, energy efficiency, etc. In proposed system for DPA, the first priority is given to farthest user i.e. target is decided as far user and to achieve this, the desired PA coefficient is calculated. After deciding the PA coefficient for far user, PA coefficient for near user is calculated based on power availability.

Assuming the rate required for far user is R*, the PA coefficients are calculated as:

From (21), $R_{2f} = \frac{B}{2}log_2\left(1 + \gamma_{2f}\right) = R^*$

$$\gamma_{2f} = 4^{R^*/B} - 1 \tag{30}$$

From (25)

$$\gamma_{2f}[(h_{2f}C_{1n})^2 P_{TE} + \sigma^2] = (h_{2f}C_{2f})^2 P_{TE} \tag{31}$$

$$(C_{2f})^2 = \frac{\gamma_{2f}(h_{2f})^2 P_{TE} + \gamma_{2f}\sigma^2}{[(h_{2f})^2 P_{TE} + \gamma_{2f}(h_{2f})^2 P_{TE}]} \tag{32}$$

From (24):

$$(C_{1n})^2 = 1 - \frac{\gamma_{2f}(h_{2f})^2 P_{TE} + \gamma_{2f}\sigma^2}{[(h_{2f})^2 P_{TE} + \gamma_{2f}(h_{2f})^2 P_{TE}]}$$

$$(C_{1n})^2 = \frac{(h_{2f})^2 P_{TE} - \gamma_{2f}\sigma^2}{[(h_{2f})^2 P_{TE} + \gamma_{2f}(h_{2f})^2 P_{TE}]} \tag{33}$$

V. Power Allocation Algorithm

The performance between static PA (SPA) and DPA is compared using the following two algorithms; fair power allocation (FPA) and modified fair power allocation (MFPA) algorithm. C_{1n} and C_{2f} are adjusted dynamically based on target rate to get the outage probability. In FPA, $(C_{2f})^2$is set in such a way that it should not exceed one. This increases outage probability with increase in target rate requirement which is expected because probability of achieving the target rate for far user becomes lower if target rate becomes higher. In addition to this, the performance of outage probability is not very satisfactory for near user after certain range of target rate. To improve the near user's outage, MFPA is used where $(C_{2f})^2$is set to zero if $\gamma_{2f} > 1$. The results using both DPA techniques are discussed in Section V.

Fair Power allocation Algorithm

1. Set the required sum rate for the far user. i.e. let's set $R_{2f} = R^*$
2. Calculate the value of power allocation coefficients; C_{2f} & C_{1n} such that $R_{2f} \geq R^*$
3. Decide the
$$(C_{2f})^2 = min\left\{1, \frac{\gamma_{2f}(h_{2f})^2 P_{TE} + \gamma_{2f}\sigma^2}{[(h_{2f})^2 P_{TE} + \gamma_{2f}(h_{2f})^2 P_{TE}]}\right\}$$
4. Calculate $(C_{1n})^2 = 1 - (C_{2f})^2$.

Modified Fair Power allocation Algorithm

1. Set the required sum rate for the far user. i.e. let's set $R_{2f} = R^*$
2. Calculate the value of power allocation coefficients; C_{2f} & C_{1n} such that $R_{2f} \geq R^*$
3. Decide the $(C_{2f})^2 = 0;\ if\ \gamma_{2f} > 1$
4. Calculate $(C_{1n})^2 = 1 - (C_{2f})^2$.

VI. Neural Network Based Detection

The NN - based NOMA VLC is shown in Fig. 3. The data transmission process remains same as discussed for a conventional NOMA VLC system in Fig. 1(a)-(b). The superposed signal received at PDs are applied after DFT operation to decode NOMA signals using the NN-algorithms: CNN, LSTM and DNN.

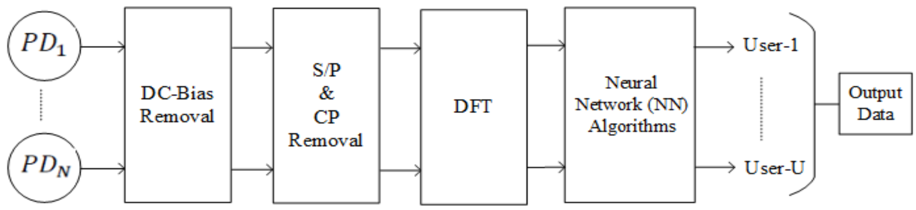

Fig. 3. NN - Based NOMA-VLC receiver

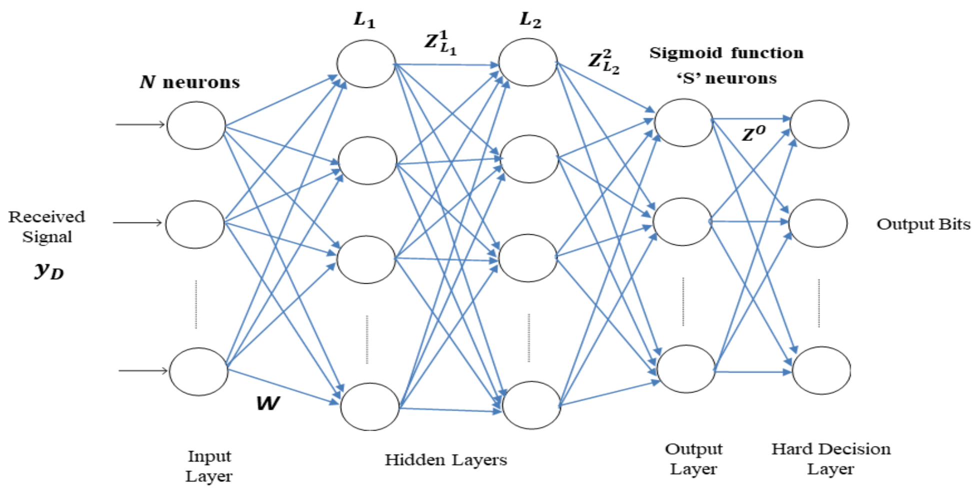

Fig. 4. General Structure of DNN

A. DNN

The general form of DNN structure is shown in Fig. 4. The structure consists of input layer, two hidden layers, one output layer and one hard decision layer. The input layer has N neurons based on the received signal at PDs and after DFT. The input signal to DNN is denoted as y_D. Two hidden layers with L_1 and L_2 are used which are connected to extract the features. Rectified linear unit (ReLU) is used as an activation function to train and to achieve better performance in NNs. Here, b and W represents the bias and weight of the hidden layers. The output of the hidden layers 1 and 2 are denoted as $Z_{L_1}^1$ and $Z_{L_2}^2$ which can be represented as:

$$Z_{L_1}^1 = f_{ReLU}(W_1\, y_D + b_1) \tag{34}$$

$$Z_{L_2}^2 = f_{ReLU}(W_2 Z_{L_1}^1 + b_2) \tag{35}$$

where $W_1 \in \mathbb{R}^{L_1 \times N}$ & $b_1 \in \mathbb{R}^{L_1}$ corresponds to hidden layer-1 and $W_2 \in \mathbb{R}^{L_2 \times L_1}$ & $b_2 \in \mathbb{R}^{L_2}$ corresponds to hidden layer-2. Also,

$$f_{ReLU}(\tau) = \max(0, \tau) \tag{36}$$

The Sigmoid function is used to estimate the bits at the output layer with S neurons in between (0, 1). The Sigmoid function is represented as:

$$f_{Sigmoid}(\tau) = \frac{1}{1+e^{-\tau}} \tag{37}$$

Hence, the estimated information bits after output layer can be represented as:

$$Z^O = f_{Sigmoid}(W_3 Z_{L_2}^2 + b_o) \tag{38}$$

$$Z^O = \{z_1^O, z_2^O, z_3^O, \dots \dots \dots, z_S^O\}^T \tag{39}$$

Finally, hard decision layer is used to receive output bits, b_s. Here, the threshold operation is performed which is mathematically represented as:

$$b_s = \begin{cases} 1, & if\ b_s^O \geq 0.5 \\ 0, & if\ b_s^O < 0.5 \end{cases} \tag{40}$$

The mean square error (MSE) is used as a loss function to find the error between received and transmitted bits.

B. CNN

The general form of CNN structure is shown in Fig. 5. Two convolution layers are used. The inputs to convolution-1 are modulated signal on N subcarriers which is represented as $y_c^1 = [y_C^R, y_C^I]$. y_C^R and y_C^I are real and imaginary part of input to CNN. According to CNN process, input convolutes with kernel with size M and followed by ReLU activation function which is implemented in the first convolution layer. The final output of convolution layer-1 is represented as:

$$Z_{L_1}^{1,i} = f_{ReLU}(y_c^i) = \max(0, Z_c^{1,i}) \tag{41}$$

where, $$Z_c^{1,i} = y_c^1 * K_1^i + b_1^i \tag{42}$$

$Z_c^{1,i}$ is the output before applying an activation function. K_1^i is i^{th} kernel of convolution layer-1 ($i = 1,2,3, \dots, M$). b_1^i is the bias with respect to kernel K_1^i.

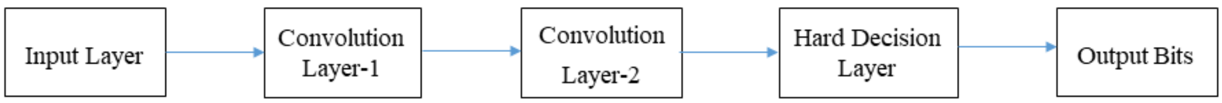

Fig. 5. General Structure of CNN

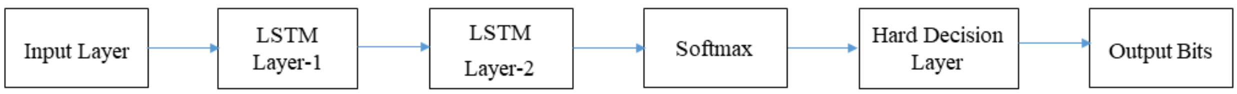

Fig. 6. General Structure of LSTM

Similarly, the output of convolution-1 is passed through convolution layer-2 which contains kernel size $2U$. Here, the Sigmoid function is used as an activation function to estimate the bits at the output of convolution layer-2 in between (0, 1). The final output of convolution layer-2 is represented as:

$$Z_{L_2}^{2,i} = sigmoid(Z_c^{2,i}) \tag{43}$$

where, $$Z_c^{2,i} = y_c^2 * K_2^i + b_2^i \tag{44}$$

y_c^2 is the input to convolution layer-2. $Z_c^{2,i}$ is the output before applying an activation function. K_2^i is i^{th} kernel of convolution layer-2 ($i = 1,2,3, \dots, 2U$). b_2^i is the bias with respect to kernel K_2^i. Next, hard decision is used as per (40) to receive the output bits. The MSE is used as a loss function to find the error between received and transmitted bits.

C. LSTM

The general form of LSTN structure is shown in Fig. 6 which consist of two LSTM layers as hidden layers. The standard LSTM unit is discussed in [18]. The input to LSTM layers are historical sequence. The output of LSTM layer-2 is denoted by y with dimension C which passes through the softmax layer. The softmax layer is an activation function used to obtain the probability of each input and the sum of all probabilities is one.

$$softmax(y) = \frac{e^{y_i}}{\sum_{j=1}^{C} e^{y_j}} \tag{45}$$

where, e^{y_i} and e^{y_j} is the standard exponential function for input and output vector. Finally, hard decision is used as per (40) to receive the output bit

VII. Results and Discussion

Following the proposed scenario as discussed in Section III, the center of the ground is considered as origin point. The conventional NOMA VLC system as shown in Fig. 1 is simulated using MATLAB R2021a. Various parameters are analyzed as discussed below. The simulation parameters are listed in Table I.

TABLE I: Simulation Parameters

Parameter	Value
LED emitter	(0,0,3)
User distance from the ground	0.75m
Users	User-1: (0, 0, 0.75) User-2: (1.8, 1.9, 0.75)
SPA coefficient	User-1 (near) : $C_{1n} = \sqrt{0.25} = 0.5$ User-2 (far) : $C_{2f} = \sqrt{0.75} = 0.87$
Semi angle of LED	60 deg.
Physical dimension of PD	1 cm^2
FOV of PD	70 deg.
Responsivity of PD	0.4 *A/W*
Modulation	4 QAM
DFT	64
CP	6
Transmission bandwidth	20MHz

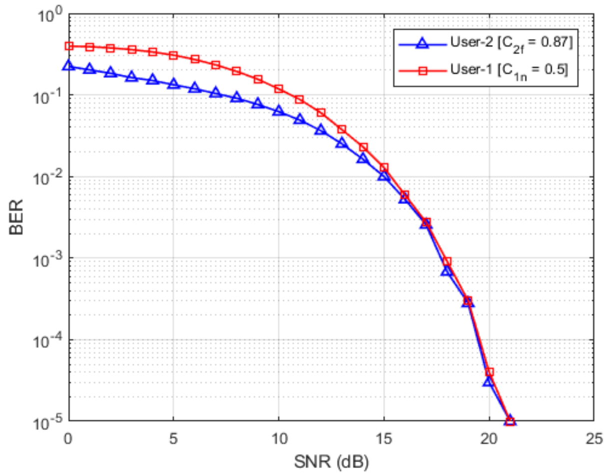

Fig. 7. SNR-BER performance

The simulation results of BER for a NOMA VLC is shown in Fig. 7. It is observed that BER performance of user-2 is slightly better than user-1 in low SNR range. This is due to SIC operation due to which User-1 has to decode user-2's data from superposed signal before decoding its own signal. If User-2's decoding is wrong then it will be an error in decoding User-1's data and thus will impact BER. Here, both user's needs approximately 21dB to obtain 10^{-5} BER.

Next, we analyzed the outage probability and achievable capacity with respect to transmitted power. The simulation result of achievable capacity in terms of transmitted power is shown in Fig. 8. R_{21} is the achievable data rate at the user 1 for decoding the user 2 signal (before SIC). The capacity increases with transmit power for user-2 but for user-1, it become almost constant. This is because, user-1 has to perform SIC before decoding its own signal whereas User-2 is far to LED emitter which get decoded first. In addition, power allocation coefficient is higher for far user. Here, R_{1n} is obtained after removing the interference from far user transmission by SIC. Further, outage probability in terms of transmitted power is plotted as shown in Fig. 9. It is observed that probability of outage for both the users are very minimum at lower value of transmit power and as power increases it reaches to zero.

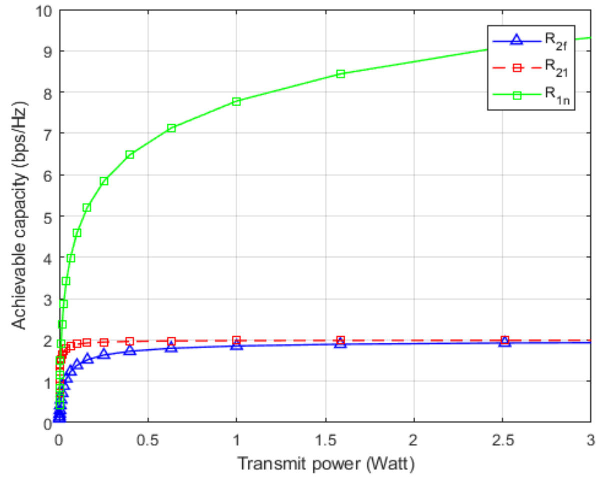

Fig. 8. Achievable capacity as a function of transmit power

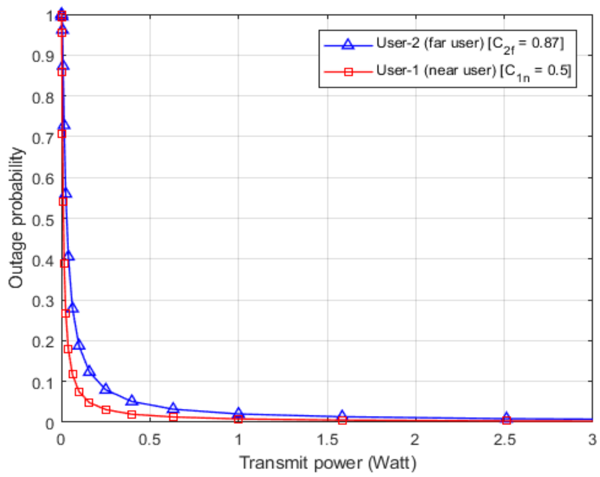

Fig. 9. Outage probability as a function of transmit power

The BER performance parameter is also analyzed with respect to transmitted power as shown in Fig. 10. The BER performance of user-1 is better than user-2 in terms of transmit power which is obvious as user-1 is near to transmitter.

The SPA is used for above parameter analysis. Further, DPA is also used to optimize the PA coefficients. The FPA and MFPA technique is implemented as discussed in

Section III B. To compare the SPA and FPA, outage probability is analyzed considering the target rate of far user. The simulation result is shown in Fig. 11. The transmitted power is set as 3W. It is observed that DPA outperforms SPA. We obtain discontinuity and very low outage probability with SPA around 20 Mbps. As observed. As observed, the outage probability for SPA saturates at 1 for far user with target rate greater than 20 Mbps. This behavior is observed because SPA does not take target requirement into consideration. Hence, SPA may not be suitable always. As C_{1n} and C_{2f} are adjusted based on target rate, thus outage probability is low in FPA. The probability of achieving the target rate for far user becomes lower as target rate increases which results in the outage of far user. At the same time, outage of near user is satisfactory for FPA in range of 60 to 90 Mbps target rate of far user. But after this, near user always in outage.

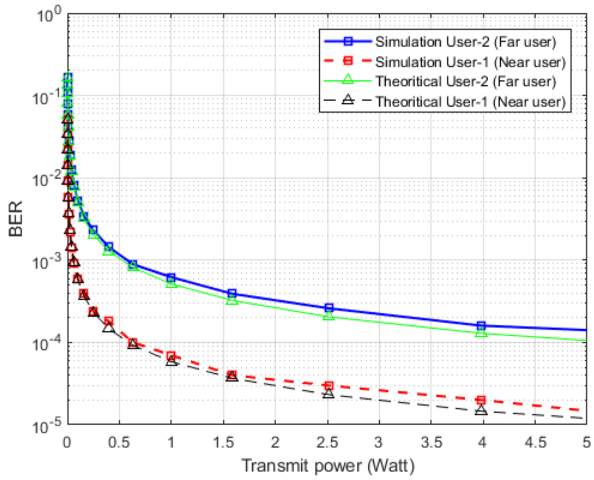

Fig. 10. BER as a function of transmit power

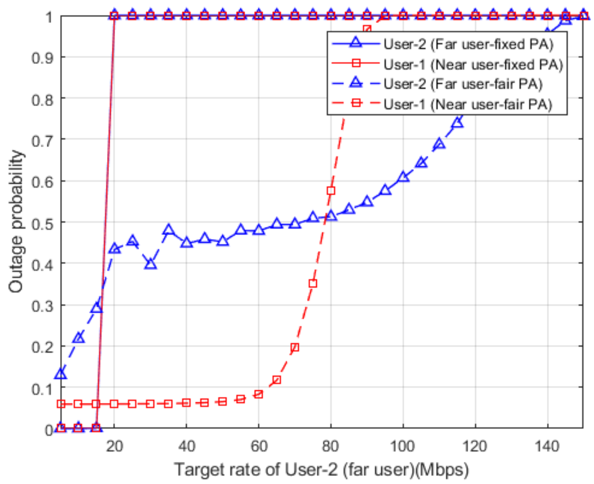

Fig. 11. Outage probability as a function of target rate of far user

To optimize the performance, MFPA is implemented. The simulation result of outage probability as a function of target rate using MFPA is shown in Fig. 12. SPA gives same performance. Also, far user performance for MFPA and FPA remains almost the same. But for near user, the performance of outage probability is improved. From the results, it is analyzed that more favor is given to far user until approximately 85 Mbps of rate by allocating more power irrespective of near user performance and, beyond 85Mbps, it goes in favor of near user instead of wasting power on far user. Thus, MFPA is just an approach to reduce the near user's outage. The PA coefficients, C_{1n} & C_{2f}, are fixed under SPA and hence the performance is independent of user's channel conditions if channel changes instantaneously. But in the DPA, C_{1n} & C_{2f} gets updated if the channel changes. This will provide a higher achievable sum rate and a lower outage in the case of DPA than SPA.

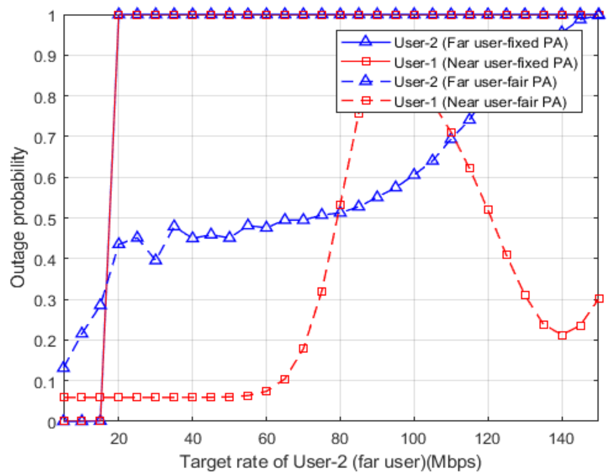

Fig. 12. Outage probability as a function of target rate of far user

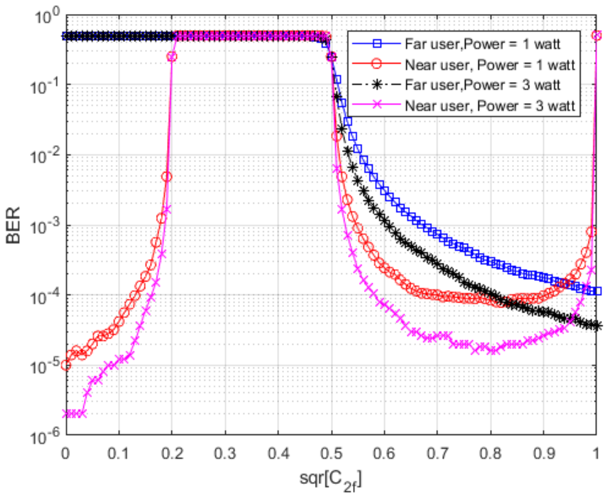

Fig. 13. BER performance as a function of PA coefficient

It is clear that PA affects the NOMA. To understand this, the BER performance is simulated in terms of PA coefficient for far user as shown in Fig. 13. Once PA coefficient is allotted for far user then PA coefficient for near user can be calculated using (31). Results are obtained when transmit power is 1W and 3W. In both the cases, there is low BER i.e. $< 10^{-4}$ for near user if $0.6 < \sqrt{C_{2f}} < 0.15$. When $\sqrt{C_{2f}}$ is close to zero then BER is low for near user because more power (almost maximum) is assigned to near user and high BER for far user. In this case, near user dominates far user. Similarly, if $\sqrt{C_{2f}}$ is close to one, then near user offers high BER. Thus, both users can provide fair performance if $\sqrt{C_{2f}}$ is in between 0.5 to 1.

NOMA performance depends on SIC. User's data is decoded if there is perfect cancellation in SIC. If there is no perfect cancellation then SIC would be imperfect which result in errors while decoding. The simulation result is obtained to analyze the effect of imperfect SIC for achievable capacity as function of transmit power considering error fraction. The Fig. 14 shows achievable data rate at user-1 with imperfect SIC. It is found that as SIC error increases, the achievable capacity performance degrades.

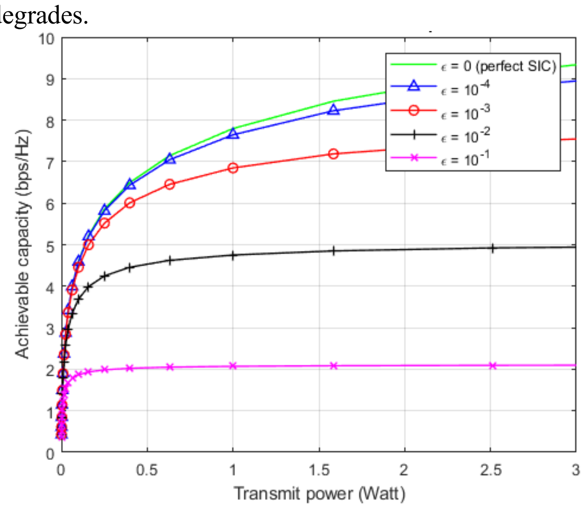

Fig. 14. Achievable data rate at user-1 with imperfect SIC

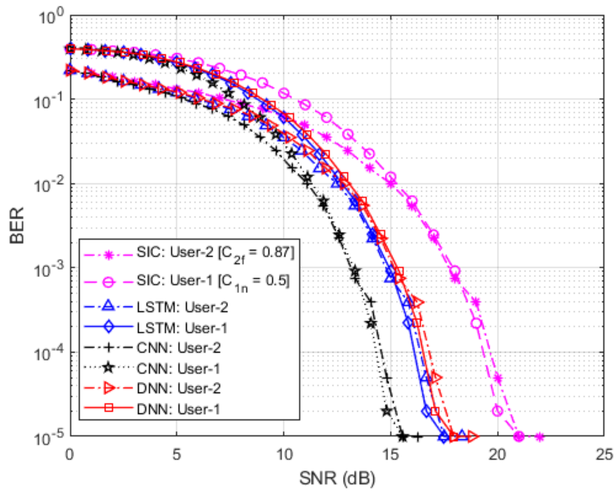

Fig. 15. BER performance as a function of SNR using NN methods

To overcome the problem of imperfect SIC and the nonlinearity in VLC, NN-based receiver is implemented. The system is analyzed using three algorithms which are DNN, CNN, and LSTM. Data sets are randomly generated in MATLAB for offline training and online deployment. In this way NN-based receiver cannot characterize the random sequences. Here, 48000 symbol which is NOMA modulated data are been used for training and for online deployment. The 70% data is used for training and 30% used for evaluation. The learning rate is 0.001. The number of neurons in each hidden layer is 16. The number of neurons in input and output layer is 4 and 24 respectively. Finally, using NN algorithms, the performance of BER is analyzed in terms of SNR using NN-based receiver as shown in Fig. 15. It is observed that NN- based receiver outperforms SIC receiver i.e. all three algorithms offers better BER-SNR performance than SIC. However, there is comparative performance variation between algorithms. It is observed that the CNN outperforms LSTM, DNN, and SIC approximately by 2dB, 2.5dB, and 5dB SNR respectively to obtain 10^{-5} BER almost for both users. The DNN and LSTM performance is slightly varied. Thus, the CNN algorithms provide comparatively a better performance. As VLC suffers nonlinear distortion due to the nonlinearity characteristics of LEDs at the transmitter, channel, and PDs at the receiver, CNN can also be seen as a better alternative solution to resolve the nonlinearity in VLC.

The BER as a function of bitrate is simulated for SIC, DNN, CNN, and LSTM using NN algorithms and result is shown in Fig. 16. The NN algorithms perform better when compared with SIC for both the users. LSTM and DNN performs almost same whereas CNN performance is better than SIC, DNN, and LSTM for both the users. Some numerical observations are shown in Table II. It is found that the percentage improvement of BER is outperformed by CNN and especially in comparison with SIC.

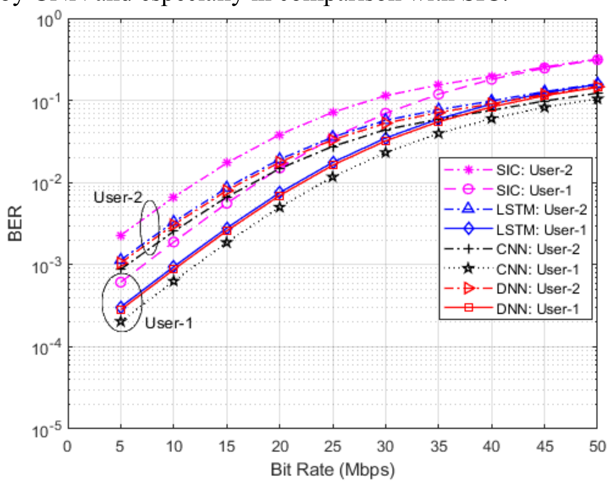

Fig. 16. BER performance as a function of bitrate using NN method

TABLE II: BER COMPARISON

Bitrate	Users	BER			
		CNN	LSTM	DNN	SIC
20 Mbps	User-1	5.015e-3	14.75e-3	14.75e-3	16.944e-3
	User-2	14.75e-3	17.7e-3	17.7e-3	38.36e-3
15 Mbps	User-1	1.86e-3	2.57e-3	2.57e-3	5.579e-3
	User-2	7.968e-3	8.632e-3	8.632e-3	17.26e-3

Further, the CNN, DNN and LSTM is also compared with respect to training time. It is found that the training time for DNN, CNN, and LSTM are 12.4325 sec, 15.1096 sec, and 27.7684 sec respectively. The speed for convergence in LSTM is slower than DNN and CNN.

CNN based NN can be used with less number of training parameters without affecting the performance. CNN can be used to reduce the number of parameters to train without sacrificing performance but training is bit slower than DNN. This is due to weight sharing and sparse connections in CNN. LSTM requires more parameters than CNN.

VIII. Conclusion

The NOMA VLC system is analyzed. PA and its coefficient factor play a significant role. The performance of NOMA using SPA and DPA is analyzed. DPA offers better achievable capacity and outage. Under DPA, FPA and MFPA is used and it is found that MFPA is suitable especially for better outage for near user. Further, the effect of imperfect SIC is analyzed which result errors in decoding. To overcome the nonlinearity effects in VLC; NN-based receiver is analyzed where three algorithms are considered such as DNN, LSTM, and CNN. All these algorithms outperform SIC based receiver and CNN outperforms LSTM, DNN, and SIC based receiver. To learn the characteristics of the channel, algorithms use transmitted signals as labels and received signals at the receiver as samples. The applications of NN in VLC compared with other area of research such as image processing are in initial stage. It is convincing to say that NN in VLC will provide promising field for future research to carry forward the VLC systems performance.

Conflict of Interest

The authors declare no conflict of interest.

Author Contributions

Mahesh Kumar Jha conducted the research work. Navin Kumar analyzed the data. Navin Kumar, Rubini P and Y. V. S. Lakshmi supervised the work as a supervisor. All authors agreed to this final version of work submission.

References

[1] T. C. Yu, W. T. Huang, W. B. Lee, C. W. Chow, S. W. Chang, and H. C. Kuo, "Visible light communication system technology review: Devices, architectures, and applications," *Crystals*, vol. 11, no. 9, p. 1098, Sep. 2021.

[2] M. W. Eltokhey, M. Khalighi, and Z. Ghassemlooy, "Multiple access techniques for VLC in large space indoor scenarios: A comparative study," in *Proc. 15th International Conference on Telecommunications*, Graz, Austria, 2019, pp. 1-6.

[3] S. S. Bawazir, P. C. Sofotasios, S. Muhaidat, Y. Al-Hammadi, and G. K. Karagiannidis, "Multiple access for visible light communications: Research challenges and future trends," in IEEE Access, vol. 6, pp. 26167-26174, 2018.

[4] L. Yin, W. O. Popoola, X. Wu, and H. Haas, "Performance evaluation of non-orthogonal multiple access in visible light communication," *IEEE Transactions on Communications*, vol. 64, no. 12, pp. 5162-5175, Dec. 2016.

[5] M. K. Jha, N. Kumar, and Y. V. S. Lakshmi, "Performance of Zero-Biased NOMA VLC System," in *Proc. IEEE 3rd 5G World Forum (5GWF)*, Bangalore, India, 2020, pp. 519-523.

[6] B. Lin, X. Tang, and Z. Ghassemlooy, "Optical power domain NOMA for visible light communications," *IEEE Wireless Communications Letters*, vol. 8, no. 4, pp. 1260-1263, Aug. 2019

[7] H. Marshoud, V. M. Kapinas, G. K. Karagiannidis, and S. Muhaidat, "Non-Orthogonal multiple access for visible light communications," *IEEE Photonics Technology Letters*, vol. 28, no. 1, pp. 51-54, Jan. 2016

[8] X. Zhang, Q. Gao, C. Gong, and Z. Xu, "User grouping and power allocation for NOMA visible light communication multi-cell networks," *IEEE Communications Letters*, vol. 21, no. 4, pp. 777-780, April 2017.

[9] Z. Dong, T. Shang, Q. Li, and T. Tang, "Differential evolution-based optimal power allocation scheme for NOMA-VLC systems," *Opt. Exp*., vol. 28, no. 15, pp. 21627-21621, Jul. 2020

[10] S. Ma, Y. He, H. Li, S. Lu, F. Zhang, and S. Li, "Optimal power allocation for mobile users in non-orthogonal multiple access visible light communication networks," in *IEEE Transactions on Communications*, vol. 67, no. 3, pp. 2233-2244, March 2019.

[11] H. Marshoud, P. C. Sofotasios, S. Muhaidat, G. K. Karagiannidis, and B. S. Sharif, "Error performance of NOMA VLC systems," in *Proc. IEEE International Conference on Communications*, Paris, France, 2017, pp. 1-6.

[12] K. Ying, Z. Yu, R. J. Baxley, H. Qian, G. K. Chang, and G. T. Zhou, "Nonlinear distortion mitigation in visible light communications," *IEEE Wireless Communications*, vol. 22, no. 2, pp. 36-45, April 2015.

[13] Y. Fan, D. Dan, Y. Li, Z. Wang, and Z. Liu, "Intelligent communication: Application of deep learning at the physical layer of communication," in *Proc. IEEE 4th Advanced Information Management, Communicates, Electronic and Automation Control Conference*, Chongqing, China, 2021, pp. 1339-1345.

[14] X. Li, Q. Gao, C. Gong, and Z. Xu, "Nonlinearity mitigation for VLC with an artificial neural network based equalizer," in *Proc. IEEE Globecom Workshops (GC Wkshps)*, Abu Dhabi, United Arab Emirates, 2018, pp. 1-6.

[15] A. Yesilkaya, O. Karatalay, A. S. Ogrenci, and E. Panayirci, "Channel estimation for visible light communications using neural networks," in *Proc. International Joint Conference on Neural Networks*, Vancouver, BC, Canada, 2016, pp. 320-325.

[16] X. Wu, Z. Huang, and Y. Ji, "Deep neural network method for channel estimation in visible light communication," *Opt. Commun.*, vol. 462, May 2020.

[17] J. M. Kahn and J. R. Barry, “Wireless infrared communications,” *Proceedings of the IEEE*, vol. 85, no. 2, pp. 265-298, Feb. 1997.
[18] K. Greff, R. K. Srivastava, J. Koutn k, B. R. Steunebrink, and J. Schmidhuber, “LSTM: A search space odyssey,” *IEEE Transactions on Neural Networks and Learning Systems*, vol. 28, no. 10, pp. 2222-2232, Oct. 2017.

Mahesh Kumar Jha was born in Ranchi, Jharkhand, India in 1985. He is working as an assistant professor in CMR Institute of Technology, Bangalore, India. He received his M.Tech degree in VLSI design and Embedded System form National Institute of Technology, Jamshedpur, India in Dec. 2011 and currently he is pursuing his Ph.D in area of Visible Light communication (Optical Wireless Communication) from Visvesvaraya Technological University, Belagavi, India. He obtained his bachelor degree in Electronics and Telecommunication engineering form Biju Patnaik University of Technology, Rourkela, India in year 2007. He has over 10 years of teaching experience. He has over 15 publications in reputed international journals and IEEE conference proceedings. He is a first rank holder in M.Tech at NIT Jamshedpur. He has also received best paper award. He is Sr. Member of IEEE. He is actively associated with IEEE ComSoc Bangalore chapter and also IEEE VTS Bangalore chapter. His research area includes Visible Light Communication, Optical Wireless Communication, MIMO-OFDM, IoT & Smart City.

Navin Kumar was born in Nalanda, Bihar, India in 1969. He serves as Chairperson and Professor at the Department of Electronics and Communication, School of Engineering, Amrita Vishwa Vidyapeetham, Bengaluru. He obtained his Ph.D. in Telecommunication Engineering from the University of Porto, Aveiro and Minho – Portugal, Europe (2007-2011) and M.Tech. in Digital System Engineering from Motilal National Institute of Technology, Allahabad, India in the year 2000. He did his bachelor’s degree in Engineering from the Institution of Electronics and Telecommunication Engineers, New Delhi in 1996. He has over 24 years of working experience in Government, Industry and academia in IT and Telecommunication area. He has over 10 years of overseas experience in teaching, research and development. He has over 100 publications in peer-reviewed international journals and IEEE conference proceedings. In addition, he has also authored a book and book chapters. His research area includes 5G (mmWave, Architecture and Massive MIMO), Intelligent Transportation Systems, Visible Light Communication, Optical Wireless Communication, IoT & Smart City and Wireless/Mobile Communications & Networks.

Rubini. P was born in 1988 in Tamilnadu, India. She is working as an Associate Professor in CMR University, Bangalore. She completed her PhD in Information Science and Engineering from Anna University Chennai. Having 12 years of experience in teaching and research. She authored a book titled "Open Source Software". She had filed patent for smart IoT applications. She has presented papers in various national and international conferences. She has published 15+ papers in various international reputed SCI journals. She is an editor and reviewer for several international journals. She is a certified Neo4J Graph Databases professional. She completed her Diploma in Advanced SQL Databases from Alison courses. Presently she is involved in developing projects using No-Sql databases for data storage and analysis in social networking and associated with consultancy projects in AI using Machine Learning techniques.

Y. V. S. Lakshmi was born in Rajahmunry, India in 1963. She received M.Sc. Engineering and Ph.D. from Electronics and Communication Department, Indian Institute of Science, Bangalore, India. She has gained more than twenty years’ experience in the Telecom Industry in Quality, Reliability, Failure Analysis, Corporate Functions, IPR, Training & Teaching, and technology marketing. She currently Heads C-BUDDHI a self-sustaining training division of C-DOT, Group Leader IPR, Marketing & Knowledge Management group (Bangalore) and Vigilance Officer at C-DOT, Bangalore, India which is engaged in development of various projects at the frontier of Telecom technology in the areas of Optical communications, Next Generation Networks and Wireless technologies. Prior to CDOT worked at ITI Ltd. Bangalore, India. She has published and presented more than 100 papers in National and International Journals of repute and at various conferences. She is member of Professional Bodies: Fellow IETE, Senior Member IEEE, Life member IMAPS, NIQR Chairperson of Women in Engineering (WIE) of IEEE, Bangalore Chapter (2015), Chair IEEE TEMS Bangalore chapter (2020).